Journal of Interdisciplinary Mathematics
ISSN: 0972-0502 (Print), ISSN: 2169-012X (Online)
Vol. 29 (2026), No. 7, pp. 2383–2392
DOI : 10.47974/JIM-2676

Implications of mass and heat absorption on the dynamics of a rotating, turbulent stream of nanofluid through a vertical plate oscillation with standardized mass diffusion and variable temperature

P. Senthamizh †
J. Ravikumar *
Department of Mathematics
Faculty of Engineering & Technology
SRM Institute of Science & Technology
Vadapalani Campus
Chennai 600026
Tamil Nadu
India

Abstract

This study addresses a closed-form remedy for the mass and heat transport properties of an unsteady flow of a spinning nanofluid across a wavy perpendicular plate with standardized mass diffusion and a fluctuating temperature. The solutions are derived for different water-based nanofluid containing Ag, Al_2O_3, TiO_2. The governing dimension-free expressions are resolved using the Laplace Transform method. The velocity profile analyzes many physical properties, including time, rotation parameters, Schmidt number, mass Grashof number, thermal Grashof number, and others.

Subject Classification: *76D05, 76R10.*

Keywords: *Nanofluid, Concentration, Heat and mass transfer, Oscillating vertical plate.*

† *ORCID-ID:* **0009-0002-1111-1593**
* *ORCID-ID:* **0000-0002-1667-8874**

† *E-mail:* **sp9687@srmist.edu.in**
* *E-mail:* **ravikumj@srmist.edu.in; (Corresponding Author)**
2ravi.j@gmail.com

1. Introduction

The discipline of heat and mass transfer employing nanofluids has been reshaped by nanotechnology. A nanofluid is created when basic fluids, like ethylene glycol oil or water, are proportionately mixed with nanoparticles, which normally have sizes between 1×10^{-3} μm and 100×10^{-3} μm. It has exclusive qualities to enhance heat transfer reducing thermal resistance and with the help of Brownian motion, strengthen the mass transfer and reducing boundary layer thickness. It plays indispensable roles in industrial, environmental and biomedical applications. The nanofluid was first proposed by Choi [1] describes the base fluid which are evenly distributed in solid nanoparticles. In the investigational work. Abu-Nada [2] has investigated the heterogenous types of nanofluids alter the flow in spaces. Geetha, Muthucumaraswamy, and Kothandapani [3] has examined the incompressible flow of a nanofluid with magnetohydrodynamics effects on a vertical plate. The proper solution for an inclined plate embedded in a revolving environment that experienced aberrations in humidity, mass propagation, and thermal emission was sought for by Ravikumar and Vijayalakshmi [4]. Muralidharan and Muthucumaraswamy [5] investigated standard heat flux and different diffusion of mass in the parabolic infinite vertical plate in the parabolic beginning infinite vertical plate. Geetha, Sharmila, and Muthucumaraswamy [6] investigated that the magnetohydrodynamic effects on a vertical plate with the transient incompressible flow of a nanofluid. Bachok, Ishak, and Pop [7] glanced into the passage through a fluid which is nano past a surface that was traversing a boundary layer and another fluid. According to research by Reddy and Sademaki [8], nanofluids have superior conductivity to ordinary fluids, and they are also more conductive than ordinary fluids. Fadugba, Ismail, and Kekana [9] looked into the work, that the Riccati -Bernoulli sub-ODE method is an effective and simple technique for obtaining traveling wave solutions of nonlinear PDEs. Non-linear equations with partial differentials can be converted into dimensionless form using the Laplace transform. This study focused on three types of nanofluids: a cluster of water and nanoparticles such as titanium dioxide (TiO_2), aluminium oxide (Al_2O_3), and silver (Ag). The analytical solutions yield governing equations. The data are shown as a graph comprising concentration, temperature, velocity profile, rotation, Schmidt number, thermal and mass Grashof number, and time.

2. Mathematical Analysis

This work examines the behavior of an incompressible endless upward plate in the presence of minute particles that rotate along the plate due to fluctuations in temperature and mass diffusion. Here we are considering three-dimensions, where z' axis is placed at right angle side and keeping the x' axis fixed and it is normal to the surface, in the similar way y' axis is normal but not fixed. The plate rotates with the fluid at a constant angular velocity of Ω' over the x' dimension. The amount of substance and thermal level next to the surface are

$C_\infty{}'$ as well as $T_\infty{}'$ at the beginning when $t' = 0$. As time t' greater than 0 approached, the plate started to move with velocity throughout its unique level. As a result, the plate's temperature increased to $T_W{}'$ and the dissolved level over the plate grew to C_w'. Table 1, [4] shows the thermal and physical properties of nanoparticles and water.

Table 1

Thermophysical characteristics of H_2O and nanoparticles [3].

Physical properties	Water/Base fluid	Ag	Al_2O_3	TiO_2
$\rho\ (kg/m3)$	997.1	10500	3970	4250
Cp	4179	235	765	686.2
K(W/mK)	0.613	429	40	8.9538
$\beta(k^{-1})$	21×10^{-5}	1.89×10^{-5}	0.85×10^{-5}	0.9×10^{-5}
Φ	0.0	0.05	0.15	0.2

The proposed governing equations under Boussinesq's approximation of traditional unsteady flow.

$$g(\rho\beta_c)_{nf}(C - C_\infty) - \rho_{nf}\left(\frac{\partial u'}{\partial t'} - 2\Omega' v'\right) = -((g(\rho\beta_T)_{nf}(T - T_\infty)) + \mu_{nf}\left(\frac{\partial^2 u}{(\partial z')^2}\right)) \tag{1}$$

$$-(\rho_{nf}\left(\frac{\partial v'}{\partial t'} + 2\Omega' u'\right) = -(\mu_{nf}\left(\frac{\partial^2 v}{(\partial z')^2}\right))) \tag{2}$$

$$(\rho\beta_c)_{nf}\frac{\partial T'}{\partial t'} = k_{nf}\frac{\partial^2 T'}{\partial z'^2} \tag{3}$$

$$\rho_{nf}\left(\frac{\partial C'}{\partial t'}\right) = D_{nf}\left(\frac{\partial^2 C'}{(\partial z')^2}\right) \tag{4}$$

where

$$\left.\begin{aligned} \mu_{nf} &= (-(\phi - 1)^{2.5})^{-1} \\ D_{nf} &= \frac{-(-1+\phi)}{-(-1-\frac{\phi}{2})} D_f \\ \rho_{nf} &= -(-\rho_f - (\phi\rho_s - \phi\rho_f)) \\ (\rho c_p)_{nf} &= (1-\phi)(\rho c_p)_f + \phi(\rho c_p)_s \\ (\rho\beta_T)_{nf} &= (\rho\beta_T)_f(1-\phi) + \phi(\rho\beta_T)_s \\ (\rho\beta_c)_{nf} &= (1-\phi)(\rho\beta_c)_f + \phi(\rho\beta_c)_s \end{aligned}\right\} \tag{5}$$

Analysing the equations (1), (2), (3) and (4) sticking to the spherical nanoparticles The Hamilton and Crosser model proposed the nanofluid of thermal conductivity.

$$K_{nf} = K_f\left[\frac{K_s + 2K_f - 2\phi(K_f - K_s)}{K_s + 2K_f + \phi(K_f - K_s)}\right] \tag{6}$$

The proposed problem's starting and ending conditions are provided by

$$\left.\begin{array}{c} T = T_{\infty,} u' = v' = 0, C = C_{\infty,} \forall\, z', t' = 0 \\ t' > 0: u' = u_0 sinw't', v' = 0, T' = T'_{\infty}\ and\ C' = C'_{\infty} \\ T' = T'_{\infty} + (T'_{w} - T'_{\infty})\text{At' at z'} = 0 \\ C' = C'_{\infty} - \text{At'}\,(-C'_{w} - C'_{\infty})\text{At' at z'} = 0 \\ u' = 0, v' = 0,, C \to C_{\infty}, T \to T_{\infty}\ as\ z' \to \infty \end{array}\right\} \tag{7}$$

Where A= $\frac{u_0^2}{v}$

Now introducing dimensionless quantities, they become

$$\left.\begin{array}{c} (\mathrm{u},\mathrm{v}) = \frac{(\mathrm{u}\prime,\mathrm{v}\prime)}{\mathrm{u_0}};\ \mathrm{t} = \frac{\mathrm{t}\prime(\mathrm{u_o})^2}{\mathrm{v_f}};\ \mathrm{z} = \frac{\mathrm{z}\prime \mathrm{u_0}}{\mathrm{v_f}} \\ \mathrm{Pr} = \frac{\mu \mathrm{c_p}}{\mathrm{K_f}}; \theta = \frac{\mathrm{T}-\mathrm{T_\infty}}{\mathrm{T_w}-\mathrm{T_\infty}}; \Omega = \frac{\Omega\prime \mathrm{v}}{\mathrm{u_0^2}};\ \mathrm{w} = \frac{\mathrm{wt}}{\mathrm{u_0^2}} \\ \mathrm{G_r} = \frac{\mathrm{g v_f}(\beta_\mathrm{T})(\mathrm{T_w}-\mathrm{T_\infty})}{\mathrm{u_0^3}};\ \mathrm{C} = \frac{\mathrm{C}-\mathrm{C_\infty}}{\mathrm{C_w}-\mathrm{C_\infty}}; \mathrm{Sc} = \frac{\mathrm{v_f}}{\mathrm{D_f}}; \\ \mathrm{G_c} = \frac{\mathrm{g v_f}(\beta_\mathrm{c})(\mathrm{C_w}-\mathrm{C_\infty})}{\mathrm{u_0^3}} \end{array}\right\} \tag{8}$$

Expressions (1) through (4) and (7) using the equation q=u+iv, a velocity of complex i=$\sqrt{(-1)}$. Utilizing identities (5), (6) and (8) results in

$$s_1(\frac{\partial q}{\partial t} + 2i\Omega \mathrm{q}) = \mathrm{s}_4\frac{\partial^2 q}{\partial z^2} + s_2 G_r \theta + s_3 G_c C \tag{9}$$

$$s_5 Pr \frac{\partial \theta}{\partial t} = \frac{\partial^2 \theta}{\partial z^2} \tag{10}$$

$$\frac{\partial C}{\partial t} = \frac{s_6}{Sc}\frac{\partial^2 C}{\partial y^2} \tag{11}$$

where

$$\left.\begin{array}{c} s_1 = (1-\ \phi) + \phi(\frac{\rho_s}{\rho_f});\ s_2\ = (1-\ \phi) +\ \phi(\frac{(\rho\beta_{T)s}}{(\rho\beta_{c)_f}}) \\ s_3 = \frac{1}{-(\phi-1)^{2.5}}; s_4 = \frac{(1-\phi)}{1+\frac{\phi}{2}};\ s_6\ = (1-\ \phi) +\ \phi(\frac{(\rho\beta_{c)s}}{(\rho\beta_{c)_f}}) \\ s_5 = -(-K_f \left[\frac{K_s + 2K_f - 2\phi(K_f - K_s)}{K_s - 2K_f - \phi(K_s + K_f)}\right]) \end{array}\right\} \tag{12}$$

The dimensionless, opening and ending conditions

$$\left.\begin{array}{c} \mathrm{C} = \mathrm{q} = \theta = 0, for\ all\ z\ and\ t \le 0 \\ t > 0: q = sinwt; \theta\ = t, C = 1\ at\ z = 0 \\ q \to 0, \theta \to 0, c \to 0\ as\ z \to \infty \end{array}\right\} \tag{13}$$

Mathematical concepts of (9), (10) and (11) of the dimensionless governing conditions (12) can be solved by (13) using the transform method of Laplace yields

$$\theta = t(1 + 2\eta^2 b) erfc(\eta\sqrt(b)) - \frac{2\eta\sqrt(b)}{\sqrt\pi}(exp(-\eta(sc)^2)) \tag{14}$$

$$C = erfc(\eta\sqrt(a)) \tag{15}$$

$$q = \frac{exp(iwt)}{2i}\{\frac{1}{2}[-exp(2\eta\sqrt(e)\sqrt(iwt+tg)erfc(\eta\sqrt(e)-\sqrt(iw*t+g*t)]$$
$$+(exp(-2\eta\sqrt(e)\sqrt(gt+iwt)erfc(\eta\sqrt(1*e)-\sqrt{-}(-iwt-gt)]\}$$
$$+\frac{exp(-iwt)}{2i}\{\frac{1}{2}[exp(2\eta\sqrt(e)\sqrt(-i*wt+gt)erfc(\eta\sqrt(e)$$
$$+\sqrt(-(iwt-g*t)]$$
$$+(exp(-2\eta\sqrt(e)\sqrt(-iwt+gt)erfc(\eta\sqrt(e)\sqrt(-wti+gt)]$$
$$+\frac{c}{d^2}[\frac{1}{2}[-exp(-2\eta\sqrt(-f)\sqrt(-gt)\ erfc*(\eta\sqrt(f)-\sqrt(gt)$$
$$+exp(2\eta\sqrt(f)\sqrt(gt)\ erfc*(\eta\sqrt(f)+\sqrt(gt))]$$
$$-\frac{c}{d}[\frac{t}{2}[exp(-2\eta\sqrt(f)\sqrt(gt)\ erfc(\eta\sqrt(f)-\sqrt(gt)$$
$$+exp(-2\eta\sqrt(f)\sqrt(gt)\ erfc(-\eta\sqrt(f)+\sqrt(g*t))]$$
$$-\frac{\eta\sqrt{(ft)}}{\sqrt{(g)}}[(exp(-2\eta\sqrt(f)\sqrt(gt)\ erfc(\eta\sqrt(f)-\sqrt(gt))$$
$$-exp(2\eta\sqrt(f)\sqrt(gt)\ erfc(\eta\sqrt(f)+\sqrt(gt))]$$
$$+\frac{c}{d^2}[\frac{exp(dt)}{2}[(exp(-2\eta\sqrt(f)\sqrt(g+d)t)erfc(\eta\sqrt(f)-\sqrt(g+d))]$$
$$+[(exp(2\eta\sqrt(f)\sqrt(g+d)t)erfc(-(-\eta\sqrt(f))-\sqrt(g+d))]$$
$$-\frac{e}{d}\{\frac{1}{2}(-exp(-2(-\eta)\sqrt(f)\sqrt(gt)\ erfc(\eta\sqrt(f)-\sqrt(gt))$$
$$+(exp(2\eta\sqrt(f)\sqrt(gt)\ erfc(\eta\sqrt(f)+\sqrt(gt))\}$$
$$+\frac{e}{d}\{[\frac{exp(dt)}{2}[(-exp(-2(-\eta)\sqrt(f)\sqrt(g+d)t)erfc(\eta\sqrt(f)-\sqrt(g+d))]$$
$$+[(exp(2\eta\sqrt(f)\sqrt(g+d)t)erfc(-(-\eta\sqrt(f)-\sqrt(g+d))]\}$$
$$-\frac{c}{d^2}erfc(-\eta\sqrt(b))+\frac{c}{d}[t(1+2\eta^2b)erfc(\eta\sqrt(b))$$
$$-\frac{2\eta\sqrt(b)}{\sqrt(\pi)}(exp(-\eta^2\mathrm{b}-\frac{c}{d^2}[\frac{exp(dt)}{2}[exp(-2\eta\sqrt(b)\sqrt(dt)\ erfc(\eta*\sqrt(b)$$
$$-\sqrt(d*t)+exp(2\eta\sqrt(b)\sqrt(dt)\ erfc(\eta\sqrt(b)+\sqrt(dt))]$$
$$+\frac{e}{d}[erfc(\sqrt(b)\eta]-\frac{e}{d}[\frac{exp(dt)}{2}[[exp(-2\eta\sqrt(b)\sqrt(dt)\ erfc(\eta\sqrt(b)$$
$$-\sqrt(dt)+exp(2\eta\sqrt(b)\sqrt(dt)\ erfc(\eta\sqrt(b)+\sqrt(dt))] \quad (16)$$

Where

$a=\frac{Sc}{L_6}$, $b=L_5pr$, $c=\frac{GrL_3}{(bL_2-L_1)}$, $d=\frac{gL_1}{bL_2-L_1}$, $e=\frac{GmL_4}{(aL_2-L_1)}$, $f=\frac{L_1}{L_2}$, $g=2i\Omega$, $\eta=\frac{z}{2\sqrt{t}}$

erfc-function of error complement.

Both error complementary function and the error function utilise complicated parameters. The following formulas are used to distinguish between the real and imaginary components of q erfc(j+ik) = erf(j) + $\frac{exp(-j^2)}{2j\pi}$ [1-cos(2jk)] + $\frac{exp(-j^2)}{2j\pi}$ [isin(2jk)] + $\frac{2exp(-j^2)}{\pi}\sum_{n=1}^{\infty}\frac{exp(-\frac{n^2}{4})}{n^2+4j^2}[f_n(j,k)+ig_n(j,k)]+\in(j,k)$

where,

$$f_m = 2j - 2jcosh(mk)cos(2jk) + msin(mik)sin(2jk),$$
$$g_m = 2jcosh(mik)sin(2jk) + msinh(mik)cos(2jk)$$
$$|\in (j,k)| \approx 10^{-16}|\mathrm{erf}(j + ik)|$$

The solutions are obtained and the results are shown graphically.

3. Results and Discussion

To analyse, the results are done for the range of values, which are associated with parameters of thermophysical. The complication of material form is offered a profound knowledge that are displayed using graphs. We examine 3 different types of nanofluids applied to titanium oxide, silver, and aluminium dioxide nanoparticles.

The nanoparticles' size can be anywhere from 0 and 0.6. The situation of $\varphi = 0$ eliminates nanoscale characteristics.

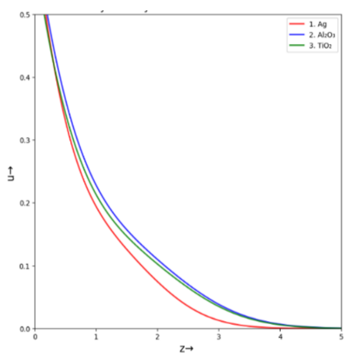

Figure 1
Primary velocity profile for different nanofluids

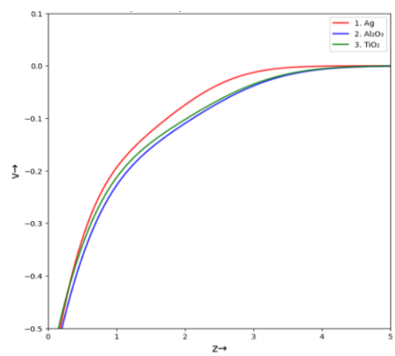

Figure 2
Secondary velocity profile for different nanofluids

The primary velocity for three types of nanoparticles are shown Figure 1. (Ag, Al_2O_3, TiO_2) and the constant proportion of solid volume as $\varphi = 0.2$, Gc = 5, Gr = 5, $Pr = 7$, Sc = 0.2, $O = 0.8$, $t = 1.0$ and $\omega t = \frac{\pi}{4}$. This analysis may be related to the similar velocity pattern observed in (Al_2O_3, TiO_2)-water, which is mainly caused by a narrower layer of boundaries correlated to the remaining particles. The secondary velocity graph for various types of nanoparticles, namely Al_2O_3 and TiO_2 and Ag are investigated. The results are displayed in Figure 2 as the values in Figure 1. When the three nanoparticles are analyzed, the velocity of Ag-water is rising while that of water is reduced.

Figure 3 depicts the velocity component 'u'(primary) with solid volume fraction as 0.2, Gr = Gc = 5 and Pr=6.2, t=0.4, $\omega t = \frac{\pi}{4}$, Sc=0.2, and it is evident that 'u' enhances as rotation (Ω) reduces. Figure 4 illustrates how the secondary velocity (v) rises in tandem with the rotation component (Ω) increasing.

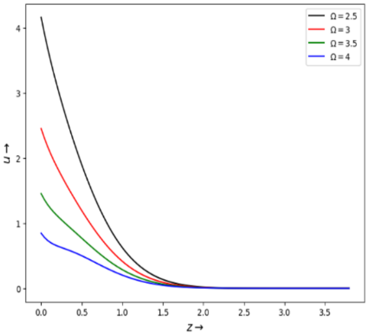

Figure 3
Primary velocity Profile for different rotation

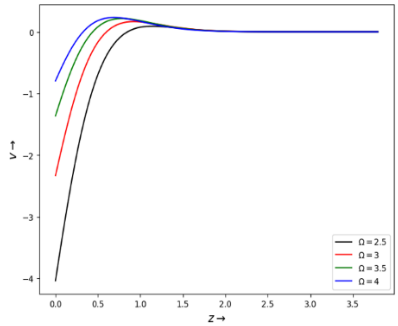

Figure 4
Secondary velocity for different rotation

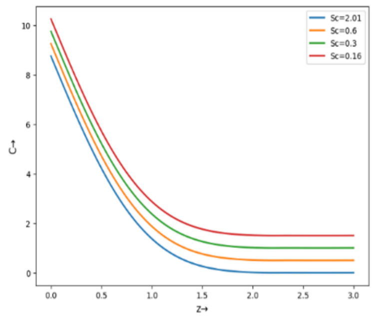

Figure 5
Concentration profile for different values of Sc

The Schmidt number contrasted with the concentration profile is shown in Figure 5. It is observed that the concentration is dropping if the value of Sc is increased.

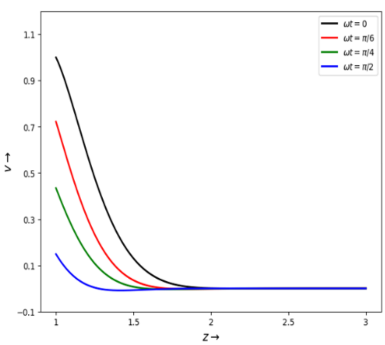

Figure 6
Primary velocity profile for different phase angle

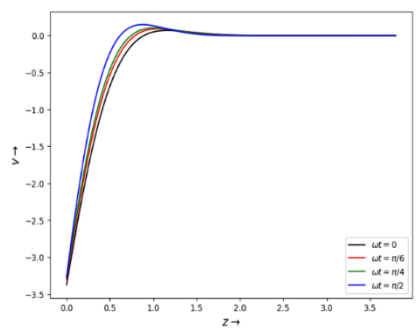

Figure 7
Secondary velocity profile for different phase angles

Figure 6 shows that when the inclination of phase angle ωt decreases, the primary component velocity (u) improves. Figure 7 depicts that due to expansion of phase angle the secondary velocity (v) also expands.

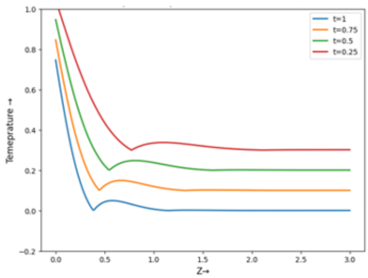

Figure 8
Temperature profile for different time(t)

Figure 8 illustrates how the TiO_2 - water nanofluid's temperature declines as time "t" advances.

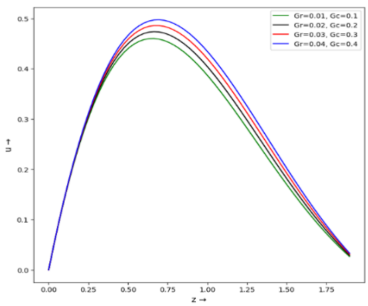

Figure 9
Primary velocity profile for different Gr and Ge values

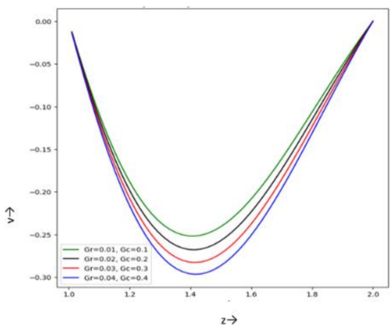

Figure 10
Secondary velocity profile for different Gr and Gc

The primary component velocity(u) profile for various Gr and Gc values is shown in Figure 9. It has been observed that rising Gr and Gc values causes the velocity to rise. Figure 10 indicates that the secondary velocity profile for distinct Gr and Gc values. It is noticed that the decreasing Gc and Gr effects the velocity to tumble downward.

4. Conclusion

This study aims to determine the precise result for the unsteady flow of nanofluids through oscillating vertical plates with standardized mass diffusion and variable temperature. Three miscellaneous types of nanofluids are considered, and the Laplace transform strategy has been used to calculate the expressions for temperature, velocity, and concentration. Using graphical representations of how multiple variables determine temperature, velocity, and concentration, a few important observations can be made.

- The primary (u) velocity rises as the angle of phase, rotation reduces and conflict with transverse velocity.
- The pattern is simply inverted with regard to the Schmidt number, but the velocity increases as the period t expands.
- Velocity of secondary (v) escalate as Gr and Gc values decrease.

Nomenclature :

Symbols	Greek Symbols and Subscripts
μ_{nf} – Dynamic viscosity of the nanofluid	β – Thermal expansion coefficient
T – Temperature	ϕ – Solid particle volume fraction
u – Velocity component in the X-direction	ω – Angular oscillation
v – Velocity component in the Y-direction	ε – Emissivity parameter
β_{nf} – Coefficient of thermal expansion of the nanofluid	μ – Dynamic viscosity
ρ_{nf} – Density of the nanofluid	σ – Stefan–Boltzmann constant
g – Acceleration due to gravity	
D_{nf} – Mass diffusion coefficient of the nanofluid	**Subscripts**
ϕ – Solid volume fraction of nanoparticles	bf – Base fluid
ρ_f – Density of the base fluid	nf – Nanofluid
μ_f – Dynamic viscosity of the base fluid	∞ – Infinity
Pr – Prandtl number	p – Particle
Sc – Schmidt number	
Gr – Thermal Grashof number	
Gc – Mass Grashof number	

References

[1] S. U. S. Choi, "Enhancing thermal conductivity of fluids with nanoparticles," in *Proc. ASME Int. Mech. Eng. Congr. Expo., Developments and Applications of Non-Newtonian Flows*, San Francisco, CA, USA, pp. 99–105 (Nov. 1995), doi: 10.1115/IMECE1995-0926.

[2] H. Abu-Nada, "Effect of nanofluid variable properties on natural convection in enclosures," *Int. J. Therm. Sci.*, vol. 49, no. 3, pp. 479–491 (2010), doi: 10.1016/j.ijthermalsci.2009.09.002.

[3] E. Geetha, R. Muthucumaraswamy, and M. Kothandapani, "Effects of thermal radiation on an unsteady nanofluid flow past over a vertical plate," *Int. J. Pure Appl. Math.*, vol. 113, no. 9, pp. 38–46 (2017).

[4] J. Ravikumar and A. R. Vijayalakshmi, "Exact solution of vertical plate in a rotating fluid with variable temperature and mass diffusion in the presence of thermal radiation," *Glob. J. Pure Appl. Math.*, vol. 12, no. 2, pp. 364–368 (2016).

[5] M. Muralidharan and R. Muthucumaraswamy, “Parabolic started flow past an infinite vertical plate with uniform heat flux and variable mass diffusion,” *Int. J. Math. Anal.*, vol. 8, no. 26, pp. 1265–1274 (2014), doi: 10.12988/ijma.2014.45143.

[6] E. Geetha, R. Sharmila, and R. Muthucumaraswamy, “Magnetohydrodynamic effects on a transient nanofluid flow past a vertical plate,” *Int. J. Mater. Sci.*, vol. 12, no. 2, pp. 85–94 (2017).

[7] N. Bachok, A. Ishak, and I. Pop, “Boundary-layer flow of nanofluids over a moving surface in a flowing fluid,” *Int. J. Therm. Sci.*, vol. 49, no. 9, pp. 1663–1668 (2010), doi: 10.1016/j.ijthermalsci.2010.01.026.

[8] B. Prabhakar Reddy and L. J. Sademaki, “A numerical study on Newtonian heating effect on heat absorbing MHD Casson flow of dissipative fluid past an oscillating vertical porous plate,” *Int. J. Math. Math. Sci.*, vol. 2022, Art. no. 7987315 (2022), doi: 10.1155/2022/7987315.

[9] S. E. Fadugba, I. Ismail, and M. Kekana, “Travelling wave solutions to the class of nonlinear partial differential equations with a Riccati–Bernoulli sub-ODE method,” *J. Interdiscip. Math.*, vol. 28, no. 7, pp. 2781–2794 (2025), doi: 10.47974/JIM-2147.

Received November, 2025